Numerical analysis of a dual-pass pumping laser with weak absorption

Guang-Ju Zhang(张光举), Ma-Li Gong(巩马理)†, and Wen-Qi Zhang(张文启)

State Key Laboratory of Tribology, Center for Photonics and Electronics, Department of Precision Instruments, Tsinghua University, Beijing 100084, *China*

(Received 14 October 2016; revised manuscript received 20 December 2016; published online 6 April 2017)

A model for a laser with dual-pass pumping is established, and an equation expressing the mode matching for this structure is presented. Through the numerical analysis of this equation, under the conditions of weak-absorption and effective absorption efficiency, the optimum radius of the pump beam waist as well as the optimum location is fitted to simple formulas, considering the quality of the pump beam, absorption coefficient, and beam waist of the cavity mode. Using these formulas, the laser with dual-pass pumping could be optimized to obtain a high slope efficiency. To test the utility of this model, an Nd:YVO_4 laser with dual-pass pumping and weak-absorption was built and optimized according to the results of the calculation. A good agreement between the results of the calculations and the experiment verified the model and the numerical analysis.

Keywords: dual-pass pimping, weak absorption, high efficiency, overlap

PACS: 02.60.Cb, 42.55.–f, 42.60.By, 42.60.Lh **DOI:** 10.1088/1674-1056/26/5/050203

1. Introduction

The recent developments in science and technology have resulted in an increasing demand for all-solid-state lasers. Several processes such as laser manufacturing, laser alignment, and laser ignition especially require all-solid-state lasers to operate with high efficiency, high output power, and high beam quality. Therefore, many researches in the field of laser technology have focused on improving the performance of all-solid-state lasers, and a couple of methods, such as mode matching and weak absorption pumping, have been developed.

Mode matching is one of the main techniques to obtain a laser with high beam quality. In this technique, the spatial distributions of the pump mode and the cavity mode will be highly overlapped in the laser crystal; thus, the fundamental-mode lasing light will be generated in the resonant cavity. In fact, the overlap efficiency that represents the quality of the mode matching also affects the overall efficiency of the laser system.[1] By now, several authors have analysed the mode matching in all-solid-state lasers. Laporta *et al.*, through the analysis of the space-dependent rate equation, reported the optimum ratio of the cavity mode size to the pump-mode size required for achieving a lower threshold and a higher output power.[2] Chen *et al.* reported their calculation of the optimum design for the laser system, with regard to the pump beam quality.[3] Their analysis indicates that the pump beam quality has a significant effect on the optimum size of the pump-mode and the corresponding location of the pump beam waist. Hajiesmaeilbaigi *et al.* conducted a numerical research on the design criteria for the laser system containing an active medium that has a small volume. Several factors including the optimum cavity mode size, pump beam quality, and minimum pump-mode size were analysed to achieve maximum output efficiency.[4] Shayeganrad *et al.* analysed the effects of the active-medium length and pump beam quality, which determines the design of the laser resonator and coupling system.[5] It should be noted that in all the reports mentioned above, the pump light was assumed to experience strong absorption within the gain medium; thus, merely the single-pass pumping was considered.

In general, a laser medium with a strong absorption of the pump light would generate heavy thermal load, which not only degrades the overall efficiency of the laser, but also threatens its safety. A widely applied solution to this problem is the adoption of weak-absorption pumping in the laser system, which ensures uniform heat distribution in the longitudinal direction of the active medium, thus reducing thermal effects such as end-effect and thermal-stress. Meanwhile, weak-absorption techniques such as in-band pumping could also improve the quantum efficiency of the laser system; thus providing the benefits of high efficiency and high output-power.[6–29] However, a laser with weak-absorption pumping faces two problems. One problem is the under-utilization of the pump power. Due to the low absorption, the pump power might not be effectively absorbed, which results in a limitation of the lasing power. The other problem arises from the mode matching of the system for a low absorption of the pump light, which, combined with the required long absorption length of the laser medium, will strongly affect the mode matching of the system. Currently, both problems are solved by applying

†Corresponding author. E-mail: gongml@mail.tsinghua.edu.cn

© 2017 Chinese Physical Society and IOP Publishing Ltd

dual-pass pumping, in which the pump power passes through the active medium twice to ensure that more pump power is absorbed. However, no numerical analysis for the dual-pass pumping laser has been reported until now.

In this paper, a model for dual-pass pumping is established and a formula for the mode-matching function, with regard to dual-pass pumping, is provided. By assuming a high absorption efficiency of 90%, numerical calculations are performed for the mode matching of the all-solid-state laser, including both dual-pass pumping and weak absorption. The calculated results provide the optimum location of the pump-mode waist and the corresponding pump-mode size for both the forward pump beam and backward pump beam. These results also indicate that these optimum values would be affected by the pump beam quality as well as by the cavity mode size. By the numerical fitting of these results, simple formulas considering the beam quality of the pumping light, absorption coefficient, and beam waist of the cavity mode are obtained to express these optimum values. These formulas would be helpful when designing the laser system. To test the utility of the model, an Nd:YVO_4 laser was built and optimized by adopting the results of the calculation and there was a good agreement between the calculation and experiment results, which verifies the model and the numerical analysis.

2. Modelling

The slope efficiency of a general all-solid-state laser can be given by[1]

$$\eta_{\text{slope}} = \frac{-\ln(1-T)}{L-\ln(1-T)}\eta_{\text{PS}}\eta_{\text{T}}\eta_{\alpha}\eta_{\text{Q}}\eta_{\text{S}}\eta_{\text{B}}. \tag{1}$$

Here, T is the transmittance of the output coupler (OC), L is the round-trip cavity loss, η_{PS} is the pump-source spectral efficiency, η_{T} is the transfer efficiency of the coupling system, η_{α} is the absorption efficiency, η_{Q} is the quantum efficiency, η_{S} is the quantum defect efficiency, and η_{B} is the overlap efficiency. η_{B} and the effective mode volume V_{eff} are co-functions of the cavity mode and the pump mode whose expression are given by[3]

$$\eta_{\text{B}} = \frac{\left(\iiint s_{\text{l}}(x,y,z)r_{\text{p}}(x,y,z)\,\mathrm{d}v\right)^2}{\iiint s_{\text{l}}^2(x,y,z)r_{\text{p}}(x,y,z)\,\mathrm{d}v}, \tag{2}$$

$$V_{eff} = \frac{1}{\iiint s_{\text{l}}(x,y,z)r_{\text{p}}(x,y,z)\,\mathrm{d}v}, \tag{3}$$

where $s_{\text{l}}(x,y,z)$ is the normalized cavity mode intensity distribution in the crystal and $r_{\text{p}}(x,y,z)$ is the normalized pump-mode intensity distribution.

For our model, $s_{\text{l}}(x,y,z)$ can be determined by assuming a fundamental mode, which is then represented as[3]

$$s_{\text{l}}(x,y,z) = \frac{2}{\pi\omega_{l0}^2 l}\exp\left(-2\frac{x^2+y^2}{\omega_{l0}^2}\right), \tag{4}$$

where ω_{l0} is the beam waist of the cavity mode, and l is the length of the medium. The relative calculation of $r_{\text{p}}(x,y,z)$ is performed by the following equation:[30]

$$r_{\text{p}}(x,y,z) = \frac{\alpha I_{\text{p}}(x,y,z)}{\eta_{\alpha}P_{\text{pf0}}}, \tag{5}$$

where α is the absorption coefficient of the pump light, and P_{pf0} is the incident pump power of the forward pump mode. The absorption efficiency η_{α}, in our model is given by $\eta_{\alpha} = 1-\exp(-2\alpha l)$. The pump intensity $I_{\text{p}}(x,y,z)$ in the medium is calculated as

$$I_{\text{p}}(x,y,z) = I_{\text{pf}}(x,y,z) + I_{\text{pb}}(x,y,z), \tag{6}$$

where $I_{\text{pf}}(x,y,z)$ is the intensity of the forward pump mode, and $I_{\text{pb}}(x,y,z)$ is the intensity of the backward pump mode. Both have similar descriptions as shown below[31]

$$I_{\text{pf}}(x,y,z) = \frac{C_{\text{pf}}}{\pi\omega_{\text{pf}}^2(z)}\exp\left(-2\frac{x^2+y^2}{\omega_{\text{pf}}^2(z)}-\alpha z\right), \tag{7}$$

$$\omega_{\text{pf}}(z) = \omega_{\text{pf0}}\sqrt{1+\left(\frac{\theta_{\text{pf0}}(z-z_{\text{pf0}})}{\omega_{\text{pf0}}}\right)^2}, \tag{8}$$

$$C_{\text{pf}} = \frac{P_{\text{pf0}}}{\iint\limits_{z=0}\frac{1}{\pi\omega_{\text{pf}}^2(z)}\exp\left(-2\frac{x^2+y^2}{\omega_{\text{pf}}^2(z)}-\alpha z\right)\mathrm{d}x\mathrm{d}y}. \tag{9}$$

For $I_{\text{pb}}(x,y,z)$, we modified the expression as

$$I_{\text{pb}}(x,y,z) = \frac{C_{\text{pb}}}{\pi\omega_{\text{pb}}^2(z)}\exp\left(-2\frac{x^2+y^2}{\omega_{\text{pb}}^2(z)}-\alpha(l-z)\right), \tag{10}$$

$$\omega_{\text{pb}}(z) = \omega_{\text{pb0}}\sqrt{1+\left(\frac{\theta_{\text{pb0}}(z-z_{\text{pb0}})}{\omega_{\text{pb0}}}\right)^2}, \tag{11}$$

$$C_{\text{pf}} = \frac{P_{\text{pf0}}\exp(-\alpha l)}{\iint\limits_{z=0}\frac{1}{\pi\omega_{\text{pb}}^2(z)}\exp\left(-2\frac{x^2+y^2}{\omega_{\text{pf}}^2(z)}-\alpha(l-z)\right)\mathrm{d}x\mathrm{d}y}. \tag{12}$$

Here, ω_{pf0} and ω_{pb0} are the radii of the pump-mode waist, while θ_{pf0} and θ_{pb0} are the corresponding far-field half-angles. z_{pf0} and z_{pb0} are the distances of the pump-mode waist from the left surface of the laser medium. It should be noted that there is a simple relationship between the radius of the pump mode and the corresponding far-field half-angles

$$\omega_{\text{pf0}}\theta_{\text{pf0}} = \omega_{\text{pb0}}\theta_{\text{pb0}} = B_{\text{PP}}, \tag{13}$$

where B_{PP} is the beam parameter product which describes the beam quality of the pump beam. The typical model for the dual-pass pumping is shown in Fig. 1.

From Eqs. (2)–(13), the expression for the mode-matching function of the single-pass pumping should be[4]

$$F_{\text{single}}(\alpha, l, \omega_{\text{l0}}, \omega_{\text{pf0}}, z_{\text{pf0}}, B_{\text{PP}})$$

$$= \frac{1}{1-\exp(-\alpha l)} \times \int_0^l \frac{\alpha\omega_{l0}^2 \exp(-\alpha z)}{\omega_{l0}^2 + \omega_{pf0}^2\left(1+\left(\frac{B_{PP}(z-z_{pf0})}{\omega_{pf0}^2}\right)^2\right)} \mathrm{d}z. \quad (14)$$

For the dual-pass pumping the function can be modified as

$$F_{dual}(\alpha, l, \omega_{l0}, \omega_{pf0}, \omega_{pb0}, z_{pf0}, z_{pb0}, B_{PP}) = \frac{1}{1-\exp(-2\alpha l)} \int_0^l \left\{ \frac{\alpha\omega_{l0}^2 \exp(-\alpha z)}{\omega_{l0}^2 + \omega_{pf0}^2\left(1+\left(\frac{B_{PP}(z-z_{pf0})}{\omega_{pf0}^2}\right)^2\right)} + \frac{\alpha\omega_{l0}^2 \exp(\alpha z - 2\alpha l)}{\omega_{l0}^2 + \omega_{pb0}^2\left(1+\left(\frac{B_{PP}(z-z_{pb0})}{\omega_{pb0}^2}\right)^2\right)} \right\} \mathrm{d}z, \quad (15)$$

which describes the spatial match between the cavity mode intensity distribution and the pump-mode intensity distribution, thus affecting the beam quality of the lasing light. Substituting Eq. (5) into Eq. (3), the overlap efficiency of the laser containing the dual-pass pumping can be expressed as

$$\eta_B = \frac{F_{dual}(\alpha, l, \omega_{l0}, \omega_{pf0}, \omega_{pb0}, z_{pf0}, z_{pb0}, B_{PP})^2}{F_{dual}(\alpha, l, \omega_{l0}/\sqrt{2}, \omega_{pf0}, \omega_{pb0}, z_{pf0}, z_{pb0}, B_{PP})}. \quad (16)$$

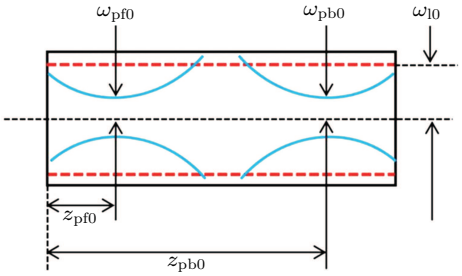


Fig. 1. (color online) Typical model for the dual-pass pumping.

3. Numerical analyses and discussion

To achieve an efficient absorption of the pump power, the absorption efficiency η_α is fixed at 90%, which is in agreement with $\alpha l \approx 1.15$. For the fixed α, l, ω_{l0}, and B_{PP}, the optimum location of the pump-mode waist ($z_{pf0.opt}$, $z_{pb0.opt}$) and the optimum radius of the waist ($\omega_{pf0.opt}$, $\omega_{pb0.opt}$) can be obtained by solving the following equations:

$$\frac{\partial F_{single}(\omega_{pf0}, z_{pf0})}{\partial \omega_{pf0}} = 0, \quad (17)$$

$$\frac{\partial F_{single}(\omega_{pf0}, z_{pf0})}{\partial z_{pf0}} = 0, \quad (18)$$

$$\frac{\partial F_{dual}(\omega_{pb0}, z_{pb0})}{\partial \omega_{pb0}}\bigg|_{\omega_{pf0.opt}, z_{pf0.opt}} = 0, \quad (19)$$

$$\frac{\partial F_{dual}(\omega_{pb0}, z_{pb0})}{\partial z_{pb0}}\bigg|_{\omega_{pf0.opt}, z_{pf0.opt}} = 0, \quad (20)$$

Figure 2 shows the plot of the optimum pump-mode radius as a function of α and B_{pp}. The radius of the cavity mode ω_{l0} is 0.5 mm. As shown by the plot, the optimum radii of the pump mode in the two directions can be regarded as identical, and they decrease with an increase in the value of α. Moreover, B_{pp} is an important factor that affects $\omega_{pf0.opt}$ and $\omega_{pb0.opt}$. Being pumped by a source with a higher beam parameter product, the laser system tends to have a larger optimum pump beam size, which is consistent with the results of the previous study.[3] Through the numerical analysis, the fitted formulas used to calculate the optimum radius of the pump beam are given by

$$\omega_{pf0.opt}, \omega_{pb0.opt} = A(B_{PP})\exp(B(B_{PP})\alpha) + C(B_{PP})\exp(D(B_{PP})\alpha), \quad (21)$$

$$A(B_{PP}) = a_1(B_{PP})^{a_2} + a_3, \quad (22)$$

$$B(B_{PP}) = b_1, \quad (23)$$

$$C(B_{PP}) = c_1(B_{PP})^{c_2} + c_3, \quad (24)$$

$$D(B_{PP}) = d_1(B_{PP})^{d_2} + d_3, \quad (25)$$

where the unit of both $\omega_{pf0.opt}$ and $\omega_{pb0.opt}$ is mm, that of B_{pp} is mm·milliradian, and that of α is cm^{-1}. A, B, C, and D are functions of B_{pp}, while their calculation factors such as a_i, c_i, d_i, and b_1 ($i = 1, 2, 3$) vary with the radius of the cavity mode as given in Table 1.

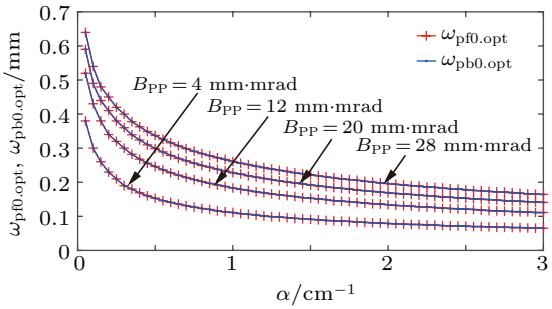


Fig. 2. (color online) Dependence of the optimum radius of the pump-mode waist on α and B_{PP}.

Figure 3 shows the optimum location of the pump-mode waist in the forward direction as a function of α and B_{pp}, while ω_{l0} was equal to 0.5 mm. It can be seen that in the range of $\alpha < 1$ cm^{-1}, $z_{pf0.opt}$ changes significantly as B_{PP} increases. However, as α increases, the effect of B_{PP} on $z_{pf0.opt}$ reduces. Figure 4 shows the relationship between $z_{pb0.opt}$ and α with a different value of B_{PP}. Compared to $z_{pf0.opt}$, $z_{pb0.opt}$ is less dependent on B_{PP}. From the numerical analysis of both $z_{pf0.opt}$ and $z_{pb0.opt}$, the following interesting but meaningful conclusion can be obtained:

$$z_{pf0.opt} + z_{pb0.opt} = l. \quad (26)$$

To simplify the calculation, we fitted $z_{\text{pf0.opt}}$ with both α and B_{PP}. The fitted formulas are

$$z_{\text{pf0.opt}} = E(B_{\text{PP}})\exp(F(B_{\text{PP}})\cdot\alpha) + G(B_{\text{PP}})\exp(H(B_{\text{PP}})\cdot\alpha), \quad (27)$$

$$E(B_{\text{PP}}) = e_1\cdot(B_{\text{PP}})^{e_2} + e_3, \quad (28)$$

$$F(B_{\text{PP}}) = f_1, \quad (29)$$

$$G(B_{\text{PP}}) = g_1\cdot(B_{\text{PP}})^{g_2} + g_3, \quad (30)$$

$$H(B_{\text{PP}}) = h_1\cdot(B_{\text{PP}})^{h_2} + h_3, \quad (31)$$

where the unit of $z_{\text{pf0.opt}}$ is mm, and the other factors, which were similar to that in the analysis for $\omega_{\text{pf0.opt}}$ and $\omega_{\text{pb0.opt}}$, are given in Table 2. Equations (21)–(31) may help in designing the laser system by adopting the dual-pass pumping, and thus the coupling system could be designed to achieve a high overlap.

Table 1. Factors for $\omega_{\text{pf0.opt}}$ and $\omega_{\text{pb0.opt}}$.

ω_{l0}/mm	a_1	a_2	a_3	b_1	c_1	c_2	c_3	d_1	d_2	d_3
0.1	0.049	0.19	0.019	–4.56	0.15	0.14	–0.080	–0.19	–0.52	–0.11
0.2	0.0069	0.61	0.13	–4.59	0.37	0.10	–0.30	–0.32	–0.22	–0.023
0.3	5.39	0.0049	–5.23	–4.71	0.69	0.084	–0.64	0.023	0.47	–0.32
0.4	–0.27	–0.13	0.48	–4.63	0.17	0.26	–0.092	2.07	0.016	–2.42
0.5	–0.44	–0.12	0.66	–4.79	0.14	0.31	–0.067	0.31	0.083	–0.66
0.6	–0.37	–0.33	0.55	–4.96	0.15	0.31	–0.077	0.070	0.23	–0.41
0.7	–0.44	–0.40	0.59	–5.10	0.13	0.35	–0.049	0.10	0.18	–0.46
0.8	–0.55	–0.30	0.74	–5.33	0.11	0.39	–0.022	–0.89	–0.035	0.51
0.9	–0.74	–0.23	0.92	–5.56	0.11	0.38	–0.028	0.59	0.045	–0.98
1.0	–0.84	–0.24	1.01	–5.72	0.12	0.38	–0.035	0.082	0.20	–0.45

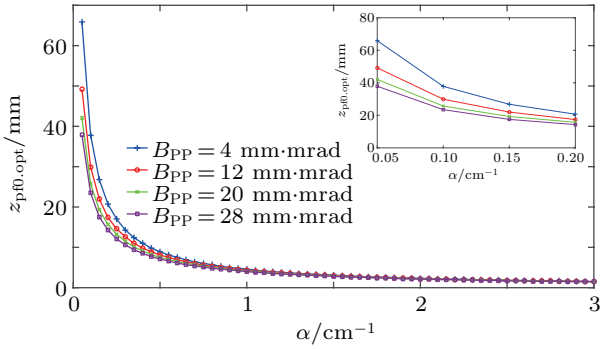


Fig. 3. (color online) Optimum distance of the forward pump beam waist as a function of α and B_{PP}.

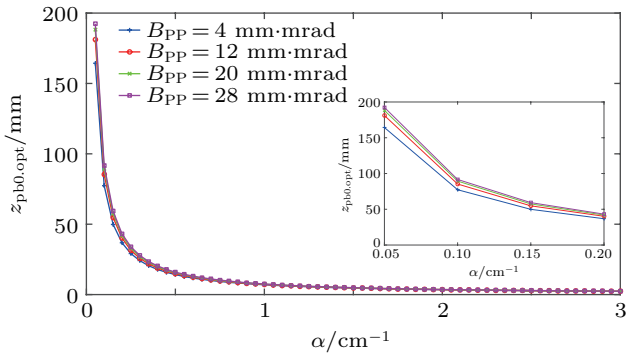


Fig. 4. (color online) Optimum distance of the backward pump beam waist as a function of α and B_{PP}.

Table 2. Factors for $z_{\text{pf0.opt}}$.

ω_{l0}/mm	e_1	e_2	e_3	f_1	g_1	g_2	g_3	h_1	h_2	h_3
0.1	47.12	−0.42	3.77	−10.09	10.47	−0.39	−0.53	−0.50	−1.14	−0.55
0.2	78.91	−0.40	4.15	−10.34	24.42	−0.13	−10.39	−0.73	−0.20	−0.24
0.3	102.7	−0.34	0.30	−10.81	−21.98	0.088	36.77	1.18	0.070	−2.17
0.4	136.2	−0.45	9.83	−10.80	−119.9	0.019	136.4	−1.32	−0.10	0.21
0.5	154.7	−0.38	4.05	−11.11	−11.91	0.13	28.31	1.49	0.056	−2.58
0.6	187.6	−0.27	−22.79	−11.37	−9.04	0.16	25.94	0.96	0.081	−2.09
0.7	224.8	−0.21	−51.72	−11.57	−14.97	0.10	32.40	12.63	0.0071	−13.78
0.8	303.9	−0.14	−126.3	−11.92	−11.70	0.12	29.48	7.68	0.012	−8.86
0.9	599.5	−0.058	−421.5	−12.20	−5.68	0.20	23.41	0.60	0.11	−1.76
1.0	−509.6	0.052	684.9	−12.46	−4.09	0.24	21.87	0.39	0.15	−1.56

Figure 5 shows the plot of Fdual as a function of α and BPP obtained by inserting the values of $\omega_{\text{pf0.opt}}$, $\omega_{\text{pb0.opt}}$, $z_{\text{pf0.opt}}$, and $z_{\text{pb0.opt}}$ in Eq. (15). For comparison, we calculated the optimum overlap function for the single-pass pumping, with a cavity mode radius of 0.5 mm, while the absorption efficiency was assumed to be 90% ($\alpha l \approx 2.3$). Obviously, the dual-pass pumping is more helpful in improving the overlap for shorter active mediums, which is especially obvious when the absorption efficient is significantly low.

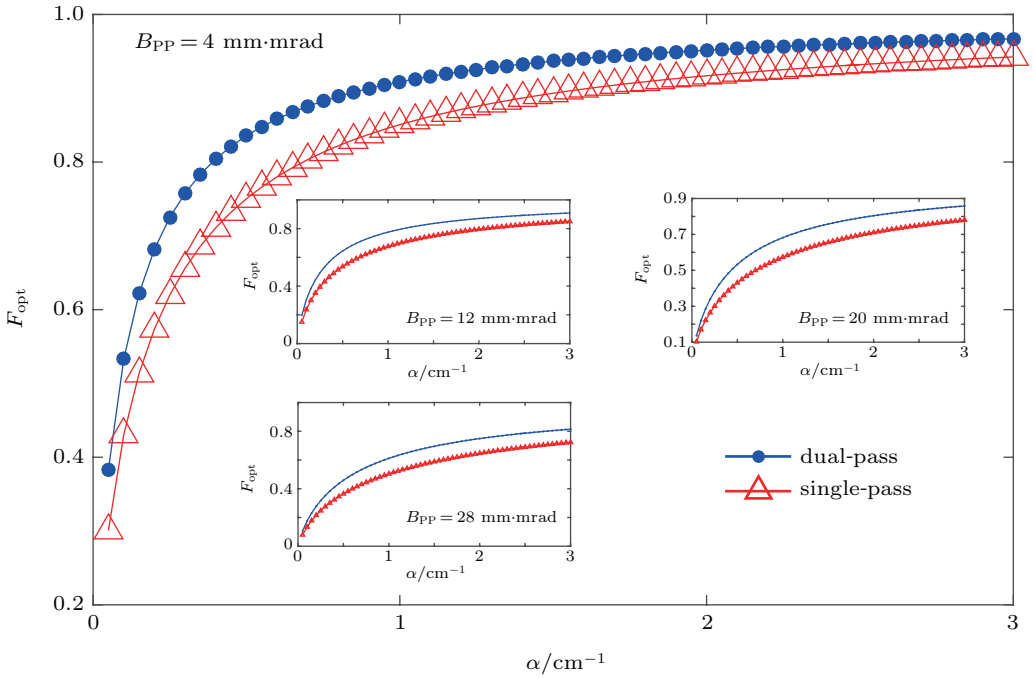


Fig. 5. (color online) Optimum mode-matching function with respect to α and B_{PP}.

4. Experiment

In order to verify the numerical analysis, an experiment was performed according to the calculations. The schematic setup for the experiment is shown in Fig. 6. The pumping source was a fibre-coupled laser diode operating at 914 nm. The coupling fibre had a diameter of 105 μm and a numerical aperture of 0.22, which resulted in a B_{PP} of ~ 5.8 mm·mrad in the laser medium. The crystal had a dimension of $1.5\times1.5\times24$ mm^3 and an Nd-doping concentration of 1%, resulting in a dual-pass absorption efficiency of $\sim 88\%$ at the pump light. Both faces of the crystal were highly transmitting (HT) at 914 nm and 1064 nm. The optical collimation system consisted of three lenses whose focal lengths were 60 mm, 60 mm, and 160 mm, respectively. M1, the plane mirror, which was HT at 914 nm and highly reflecting (HR) at 1064 nm, served as one of the cavity mirror in the laser. M2 was a plane mirror, which was HT at 914 nm and HR at 1064 nm in a 45° direction. The OC was a plane mirror whose transmittance was 52.11% at 1064 nm. After transmitting through the laser medium, the remaining pump light could be reflected back to the Nd:YVO_4 crystal by the curved mirror M3, which had a radius of 100 mm and was HR coated at 914 nm. The laser cavity had a symmetric structure whose optical length was approximately 168 mm. This resulted in a fundamental-mode spot radius of ~ 0.22 mm for the 1064-nm oscillating beam in the laser medium. From the numerical analysis for the model, the optimization values for the pump light were obtained as $\omega_{pf0} = \omega_{pb0} = \sim 0.15$ mm, $z_{pf0} = \sim 7$ mm, and $z_{pb0} = \sim 17$ mm. After these values were adopted, the relationship between the output power and the incident pump power was drawn, as shown in Fig. 7. It can be seen that the output power increases linearly with the increase in incident pump power, which resulted in a slope efficiency of $\sim 44\%$. This fits well with the numerical calculation of $\sim 45.2\%$, which was obtained by substituting the adopted and calculated values as well as $L \approx 0.06$ into Eqs. (1), (13), and (16), and this verifies both the model and the numerical method. The three factors η_T, η_Q, and η_{PS} were all regarded as ~ 1,[21,32] and the optimized overlap efficiency was obtained as 0.65.

It should be noted that in both the modelling and the experiment, the phase aberration, which is caused by the thermal lens and would result in degradation of the beam quality of the laser, was not taken into account. In general, to obtain a high-beam-quality laser, the ratio of the oscillating-beam spot radius to that of the pump light is always determined as some value.[33] Our further research would analyse the phase aberration and study its influence on the dual-pass pumping laser as well as the corresponding optimization.

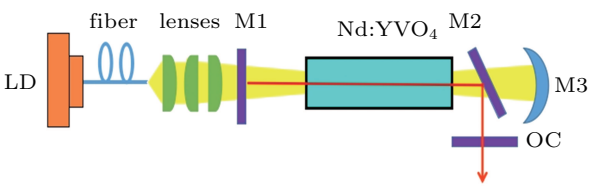


Fig. 6. (color online) Experimental setup of the Nd:YVO_4 laser with dual-pass pumping. LD: laser diode; OC: output coupler.

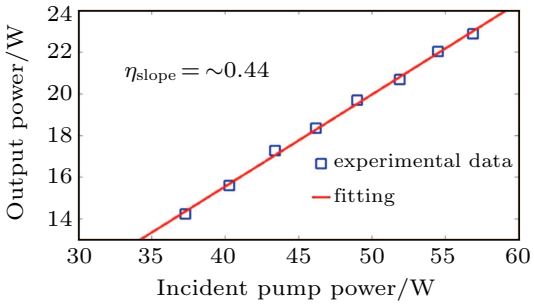


Fig. 7. (color online) Output power versus incident pump power.

5. Conclusion

In conclusion, a model for a laser containing both dual-pass pumping and weak absorption was established. Numerical analysis was performed on the mode matching between the pump mode and the cavity mode. Through numerical calculations based on effective absorption, the optimum radius of the pump beam waist and the corresponding location was fitted to simple formulas. These, including the modelling and the numerical analysis could be helpful in the design of laser system that can achieve a high overlap. An Nd:YVO_4 laser was built and optimized by adopting the results of the calculation, and there was a good agreement between the results of the calculation and the experiment, which verified the model and the numerical method.

References

[1] Koechner W 2005 *Solid State Laser Engineering*, 5th edn. (New York: Springer-Verlag) pp. 105–106
[2] Laporta P and Brussard M 1991 *IEEE J. Quantum Electron.* **27** 2319
[3] Chen Y F, Liao T S, Kao C F, Huang T M, Lin K H and Wang S C 1996 *IEEE J. Quantum Electron.* **32** 517
[4] Hajiesmaeilbagi F, Koohian A and Mahdizadeh M 2002 *J. Opt. A* **4** 52
[5] Shayeganrad G and Mashhadi L 2008 *J. Opt. A* **47** 619
[6] Zhang W, Wang F, Liu Q and Gong M 2016 *Chin. Phys. B* **25** 024207
[7] Lupei V, Pavel N and Taira T 2002 *Appl. Phys. Lett.* **80** 4309
[8] Lupei V, Pavel N and Taira T 2002 *Appl. Phys. Lett.* **81** 2677
[9] Frede M, Wilhelm R and Kracht D 2016 *Opt. Lett.* **31** 3618
[10] Pavel N, Lupei V, Saikawa J, Taira T and Kan H 2006 *Appl. Phys. B* **82** 599
[11] Pavel N, Lupei V and Taira V 2005 *Opt. Express* **13** 7948
[12] Lee H, Byeon S and Lukashev A 2012 *Opt. Lett.* **37** 1160
[13] Ding X, Chen N, Sheng Q, Yu X Y, Xu X Y, Wen W Q, Zhou R, Wang P and Yao J Q 2009 *Chin. Phys. Lett.* **26** 094207
[14] Gao J, Dai X, Zhang L and Wu X 2013 *Laser Phys. Lett.* **10** 015802
[15] Lu Y, Xia J and Zhang X 2010 *Laser Phys.* **20** 766
[16] Goldring S and Lavi R 2008 *Opt. Lett.* **33** 669
[17] Sangla D, Balembois F and Georges P 2009 *Opt. Express* **17** 10091
[18] Ding X, Yin S J, Shi C P, Li X, Li B, Sheng Q, Yu X Y, Wen W Q and Yao J Q 2011 *Opt. Express* **19** 14315
[19] Lin H, Li J and Liang X 2012 *Opt. Lett.* **37** 2634
[20] McDonagh L and Wallenstein R 2006 *Opt. Lett.* **31** 3297
[21] Sangla D, Castaing M, Balembois F and Georges P 2009 *Opt. Lett.* **34** 2159
[22] Kim J, Mackenzie J, Hayes J and Clarkson W 2012 *Opt. Lett.* **37** 1463
[23] Zhang X, Liu J, Shen D, Yang X, Tang D and Fan D 2013 *IEEE Photon. Tech. Lett.* **25** 1294
[24] Sha J, Shen D, Zhao T and Yang X 2013 *Laser Phys. Lett.* **10** 075801
[25] Lancaster D, Stevens V, Michaud-Belleau V, Gross S, Fuerbach A and Monro T 2015 *Opt. Express* **23** 32664
[26] Yao B, Cui Z, Wang J, Duan X, Dai T, Du Y, Yuan J and Liu W 2015 *Laser Phys. Lett.* **12** 025002
[27] Yuan J H, Yao B Q, Duan X M, Shen Y J, Cui Z, Yu K K, Li J and Pan Y B 2014 *Chin. Phys. Lett.* **31** 124205
[28] Fan L, Zhao W Q, Qiao X, Xia C Q, Wang L C, Fan H B and Shen M Y 2016 *Chin. Phys. B* **25** 114207
[29] Li B, Lei P, Sun B and Bai Y B 2017 *Chin. Phys. B* **26** 024206
[30] Bjurshagen S 2015 *Diode-pumped Rare-earth-doped Quasi-three-level Lasers* (Ph.D. Dissertation) (Stockholm: Royal Institute of Technology)
[31] Peng X P, Liu Q, Fu X, Chen H, Gong M and Wang D 2009 *Opt. Express* **17** 21956
[32] Brown D C, Nelson R and Billings L 1997 *Appl. Opt.* **36** 1879
[33] Hodgson H, Griswold K, Jordan W, Knapp S L, Peirce A A, Pohaiski C C, Cheng E, Cole J, Dudley D R, Petersen A B and Nighanjr W L 1999 *Proc. SPIE* 3611, *Laser Resonators II,* May 24, 1999, San Jose, USA, p. 119